

Langevin method for a continuous stochastic car-following model and its stability conditions

D. Ngoduy^{a,*}, S. Lee^a, M. Treiber^b, M. Keyvan-Ekbatani^a, H.L. Vu^c

^a*Connected Traffic Systems Lab, Dept. Civil and Natural Resources Eng., University of Canterbury, NZ*

^b*Institute for Transport & Economics, Technical University of Dresden, Germany*

^c*Institute of Transport Studies, Monash University, Australia*

Abstract

In car-following models, the driver reacts according to his physical and psychological abilities which may change over time. However, most car-following models are deterministic and do not capture the stochastic nature of human perception. It is expected that purely deterministic traffic models may produce unrealistic results due to the stochastic driving behaviors of drivers. This paper is devoted to the development of a distinct car-following model where a stochastic process is adopted to describe the time-varying random acceleration which essentially reflects the random individual perception of driver behavior with respect to the leading vehicle over time. In particular, we apply coupled Langevin equations to model complex human driver behavior. In the proposed model, an extended Cox-Ingersoll-Ross (CIR) stochastic process will be used to describe the stochastic speed of the follower in response to the stimulus of the leader. An important property of the extended CIR process is to enhance the non-negative properties of the stochastic traffic variables (e.g. non-negative speed) for any arbitrary model parameters. Based on stochastic process theories, we derive stochastic linear stability conditions which, for the first time, theoretically capture the effect of the random parameter on traffic instabilities. Our stability results conform to the empirical results that the traffic instability is related to the stochastic nature of traffic flow at the low speed conditions, even when traffic is deemed to be stable from deterministic models.

Keywords:

stochastic traffic flow, stochastic process, car-following, optimal velocity model (OVM), Langevin equations

1. Introduction

To date, there have been impressive advances in modeling the traffic-flow dynamics at both microscopic and macroscopic level. However, a majority of existing models are deterministic and fail to describe the existing uncertainty in human perception and driving behavior. These uncertainties are, among many factors, affecting the formation and propagation of stop-and-go waves (Yeo and Skabardonis, 2009). Recent studies have shown that the stochasticity is a result of many features observed in real-life traffic. For example, the concave and stochastic growth patterns of

*Corresponding author. email:dong.ngoduy@canterbury.ac.nz

oscillations are not captured by most deterministic models (Tian et al., 2016b). Emerging technologies in data collection allow us to study the true dynamics of car-following patterns which are not observed by in-situ observations of traffic flow on road. Extensive experiment results in Jiang et al. (2018) have indicated that the interplay between stochastic factors and speed adaptation is vital in the formation and evolution of oscillations. The authors have argued that the traffic instability might be determined by the competition between stochastic factors and the speed adaptation effect. This leads some implications to traffic flow theory: as deterministic models are not able to reproduce such instabilities, many efforts have been taken to develop stochastic models to capture the random human behavior over time.

At the macroscopic level, which describes the dynamics of traffic flow at an aggregated level of the detail, the stochastic properties of traffic flow have been captured well via the modified fundamental diagrams (i.e. stochastic flow-density relationships). For example, Sumalee et al. (2011) have added random noises in the model parameters of a Stochastic Cell Transmission Model (SCTM) while Zhong et al. (2013) have extended the SCTM for the traffic networks with uncertainties in supply and demand. Ngoduy (2011) has adopted a stochastic fundamental diagram in a multi-class LWR model by adding a random noise in the capacity using Gama distribution. Li et al. (2012) have also considered a stochastic fundamental diagram by adding local noises to the model parameters. Tordeux et al. (2014) used a distinct stochastic jump process for the LWR model. Basically, these methods deal with the uncertainties numerically by adding noise with known probability distributions directly to the discrete model. Recently, Laval and Chilukuri (2013) have proposed a novel method to enable an analytical stochastic solution of a class of stochastic LWR models with both stochastic initial conditions and stochastic fundamental diagram. Jabari and Liu (2012, 2013) have considered the source of randomness in the LWR model by the uncertainty inherent in a driver gap choice, which is represented by random state dependent vehicle time headway. In this model, the problem of negative sample paths of the stochastic variables is well tackled.

Microscopic models, on the other hand, describe the dynamics of traffic flow at a high level of the detail, such as the movement of individual vehicles longitudinally and laterally, i.e. car-following models and lane-changing models, respectively. Car-following models have been used widely to study the reaction of the driver with respect to his/her neighboring vehicles including the individual speed and acceleration/deceleration (see details in the book of Treiber and Kesting (2013)). In this microscopic approach, Laval et al. (2014) proposed a stochastic desired acceleration model which was extended from the car-following of Newell (2002) by adding white noise to the driver's desired acceleration. It has been reported that this model can replicate traffic oscillations. Treiber et al. (2006) argued that the desired time gap in a car-following model (i.e. the Intelligent Driver Model-IDM) is traffic state dependent, e.g. it is increased after a long time in congested traffic. The authors have modeled the desired time gap as a dynamical function of the speed variance and then replaced it in the IDM to replicate many interesting traffic phenomena: widely scattered flows, capacity drop, etc. Based on Newell's car-following model (Newell, 2002), Jabari et al. (2014) have derived a (first order) macroscopic traffic model with a probabilistic fundamental diagram. A Lagrangian version of such model has been proposed in Jabari et al. (2018), which represent the uncertain choice of the follower's free-speed, reaction times and safe distance with respect to the leader. An integrated recurrent neural network and the IDM has been proposed to predict traffic oscillations by Zhou et al. (2017). Tian et al. (2016a) have attempted to improve the IDM by considering the difference between the driving behaviors at high-speed and low-speed. More

specifically, the desired time gap is defined as a discrete function as below:

$$T(t + \Delta t) = \begin{cases} T_1 + rT_2, & \text{with probability } p \\ T(t) & \text{otherwise} \end{cases} \quad (1)$$

where r is the uniformly distributed random number between 0 and 1. T_1 and T_2 are constants indicating the range of time gap variations, typically $T_1 < T_2$. Δt is a simulation time step. The authors have shown that the proposed discrete IDM with the randomized desired time gap in equation (1) can replicate the synchronized traffic flow patterns. Latter on this improved model has been used by Tian et al. (2016b) to simulate a concave growth of traffic oscillations.

In general, it has been shown that allowing the desired time-headway to change over time (e.g. Tian et al. (2016a)) or adding noise to the continuous driver's desired acceleration (e.g. Laval et al. (2014)) have led to better model prediction. Along with this line, we aim to extend the model of Laval et al. (2014) to the form of coupled continuous stochastic differential equations which essentially captures the time-varying random choice of the driver's acceleration. The continuous form of the proposed model allows a theoretical insight into the effect of stochasticity on the stability of the traffic flow. This would help reveal quantitative relationships between car-following model structures and traffic oscillations due to uncertainties and stochasticity that are inherent from human car-following behavior. To the best of our knowledge, the stochastic stability analysis of a car-following model has only been conducted by Treiber and Kesting (2017), which only focuses on two consecutive vehicles of a specific car-following law adapted from an acceleration-based model and only provides analytical results for a sub-critical regime. It is found that stochasticity, in fact, adds nothing different to linear stability. However, a more general method and theoretical insights into the instabilities through a stream of vehicles (e.g. string stability) are still missing for general stochastic car-following models. Our approach advances the model of Laval et al. (2014) and Treiber and Kesting (2017) as following:

- We apply coupled Langevin equations to model the complex human driver behavior in aggregate lane car-following models which have a tractable mathematical foundation. In our model, an extended Cox-Ingersoll-Ross (CIR) stochastic process will be used to describe the stochastic human perception. An important property of the extended CIR stochastic process is to enhance the non-negative properties of the stochastic traffic variables (e.g. individual-speed) for any arbitrary model parameters, which is not always the case in the model of Laval et al. (2014), Yuan et al. (2018).
- We derive general (string) stochastic linear stability conditions using the proposed model. These conditions are a first attempt to show analytically how the stochasticity affects the instabilities of traffic flow. More specifically, the derived conditions are able to describe the speed variations of the followers according to certain random human behaviors given the leading vehicle's speed. This paper thus fills the methodological gap of linear stability analysis for stochastic car-following models. The results complement the traditional stability conditions for deterministic car-following models, which have been used widely in the literature. More especially, our analytical results conform to the empirical results of the traffic instability in Jiang et al. (2018). Our model shows that stochasticity does affect the stability of traffic flow at low-speed whereas the deterministic counterpart of the model shows a stable condition (i.e. Figures 1 - 3).

- The proposed model is verified against real-life traffic data (e.g. NGSIM trajectory data). The calibrated results show a good model performance.

The rest of this paper is organized as follows. Section 2 describes the model formulation and discusses some important properties of the proposed model. We derive the stochastic linear stability conditions of the proposed model in Section 3. Section 4 describes some numerical results supporting the stochastic stability conditions found in Section 3 and verifies the performance of the proposed model using NGSIM data. Finally, we conclude the paper in Section 5.

Notation

Index

t Time instant (s)

Model variables

x_n Location of vehicle n (m)

v_n Speed of vehicle n (m/s)

Δv_n Relative speed of vehicle n and its leader ($n - 1$) (m/s)

s_n Bumper-to-bumper space gap between vehicle n and its leader ($n - 1$) (m)

Model parameters

v_0 Desired speed (m/s)

s_c Critical headway (m)

α Dimensionless constant coefficient

β Reaction coefficient ($1/s$)

σ_0 Dissipation coefficient (\sqrt{m}/s for our model)

2. Model formulation

The use of multiplicative Gaussian white noise to describe the the acceleration/deceleration of the follower with respect to the leader in a car-following model has been justified in Laval et al. (2014). This was based on authors' collected data containing the position, speed, acceleration and altitude information. The data was collected during the acceleration process at signalized intersections, and corresponds to instances where the vehicle was the leader of the platoon.

This paper adopts the Langevin equations to describe the stochastic driving behavior of the car-following models. In principle, the Langevin equations are used to illustrate the stochastic process in physics, which is an effective method for the modelling of quasi-continuous diffusion processes (Mahnke et al., 2009). This formalism has been used in a wide range of problems of Brownian motions, economics and financial mathematics, chemical reactions, and diverse optimization in the last decades. Moreover, a random characteristic of the variance in the modelling of stochastic dynamics has been actively used in financial modelling. This provides the possibility of considering efficiently unpredictable and uncontrolled effects of exogenous variables, called as a stochastic volatility.

To apply such Langevin method to our traffic problems, a generic stochastic equation for the acceleration of a vehicle n includes a deterministic part and a Langevin source.

$$dv_n(t) = f(v_n(t), s_n(t), \Delta v_n(t)) dt + g(v_n(t), s_n(t), \eta(t)) dt \quad (2)$$

where $f(\cdot)$ denotes a deterministic function depending on the state of the considered vehicle and the leading vehicle while $g(\cdot)$ denotes the stochastic source which depends on only the state of the

considered vehicle and the stochastic process $\eta(t)$. When $g(\cdot) = 0$ we obtain a deterministic car-following model governed by a specific definition of the function $f(\cdot)$ such as the OVM (Bando et al., 1995), FVDM (Jiang et al., 2002) or IDM (Treiber et al., 2005). Without loss of generality, in this paper, we use the OVM as a specific definition of the function $f(\cdot)$. In fact, we have chosen the OVM as specific underlying model since it is best suited for analytic investigations. The actual contribution is the stochastic part which can be applied to a wide class of deterministic car-following models, e.g., for the IDM which will not lead to crashes, even in the linearly unstable regime. To avoid a negative gaps in the numerical implementation due to the choice of OVM, we set any negative gap to a small positive value. The function $f(\cdot)$ thus reads:

$$f(v_n(t), s_n(t), \Delta v_n(t)) = \beta [V_{op}(s_n(t)) - v_n(t)] \quad (3)$$

where $V_{op}(\cdot)$ denotes the headway-dependent optimal speed. In this paper we adopt the following functional optimal speed:

$$V_{op}(s) = \frac{v_0}{2} \left[\tanh\left(\frac{s}{s_c} - \alpha\right) + \tanh\alpha \right] \quad (4)$$

To take into account the stochastic part $g(\cdot)$, the multiplicative Gaussian white noise is used so that the model equation (2) reads:

$$dv_n(t) = \beta [V_{op}(s_n(t)) - v_n(t)] dt + \sigma(v_n(t)) dW_n(t) \quad (5)$$

where $W_n(t)$ follows a Wiener process modelling the random deviations from the mean speed of the individual vehicle. $\sigma(v_n)$ is a positive speed dependent dissipation parameter describing the noise strength. Higher $\sigma(v_n)$ implies more randomness in the acceleration of the follower.

In Laval et al. (2014), $V_{op}(s_n(t)) = v_c$ and $\sigma(v_n) = \sigma_0$ where v_c is a target speed (the constant value measured from data) and σ_0 is a constant. This linear model is essentially an Ornstein-Uhlenbeck (OU) process (Uhlenbeck and Ornstein, 1930) in which the solution for $v_n(t)$ (can be found in any stochastic differential equations textbook, e.g. Evans (2014), Gardiner (2009), Mao (2008), has the Gaussian distribution with asymptotic mean and variance:

$$E[v_n(t)] = v_0 e^{-\beta t} + v_c (1 - e^{-\beta t}) \quad (6)$$

$$Var[v_n(t)] = \frac{\sigma_0^2}{2\beta} (1 - e^{-2\beta t}) \quad (7)$$

It is obvious that at the equilibrium state:

$$\lim_{t \rightarrow \infty} E[v_n(t)] = v_c; \quad \lim_{t \rightarrow \infty} Var[v_n(t)] = \frac{\sigma_0^2}{2\beta} \quad (8)$$

Therefore, at the equilibrium state the speed variance depends only on the model parameters (i.e. σ_0 and β).

The model is simply linear but can replicate well the data observations as described in Laval et al. (2014). However, a problem in the above model type is that when the speed is low or the constant value of σ_0 is high (above the pre-determined upper bound) we could obtain negative values of speed. This is not avoidable due to the nature of the model although ones can set the speed to zero in the numerical implementation if it is negative.

A revised version of Laval et al. (2014), developed by Yuan et al. (2018), accounts for the speed-dependence of the acceleration variance:

$$dv_n(t) = \beta (v_c - v_n(t)) dt + \sigma_0 (v_c - v_n(t)) dW_n(t) \quad (9)$$

The solution for $v_n(t)$ of this model follows log-normal distribution with asymptotic mean and variance:

$$E[v_n(t)] = v_c - (v_c - v_0) e^{-\beta t} \quad (10)$$

$$Var[v_n(t)] = (v_c - v_0)^2 \left(e^{-(2\beta - \sigma_0^2)t} - e^{-2\beta t} \right) \quad (11)$$

Nevertheless, in the above models, the optimal speed of the deterministic part (i.e. drift term) is fixed to a constant or free-speed value, which limits the model performance in many cases. More specially, the above models cannot show how the stochasticity affects the instabilities in a range of traffic situations. To this end, we propose an extended and more generalized model which:

- relaxes the assumption of the constant dissipation parameter,
- uses a state-dependent optimal speed,
- enhances the non-negative properties of the speed for arbitrary values of the model parameters, and
- allows the derivation of generic string stochastic stability conditions of traffic flow.

To this end, we propose an extended Cox-Ingersoll-Ross (CIR) process (Cox et al., 1985) to model the acceleration deviations:

$$dv_n(t) = \beta [V_{op}(s_n(t)) - v_n(t)] dt + \sigma_0 \sqrt{v_n(t)} dW_n(t) \quad (12)$$

An important and distinct property of the extended CIR process over the OU process lies in the variable-dependent standard deviation factor $\sigma_0 \sqrt{v_n(t)}$, which attempts to avoid the negative trajectories of the stochastic variable $v_n(t)$ for any arbitrary values of σ_0 . More generally, when $v_n(t)$ is close to zero, the standard deviation $\sigma_0 \sqrt{v_n(t)}$ becomes very small even for high values of σ_0 , which reduces the effect of the random oscillation on the speed. Consequently, when the speed is close to zero, its evolution becomes dominated by the drift term (i.e. the deterministic part), which pushes the speed towards the (positive) value V_{op} . It is worth mentioning here that in the OVM, when traffic becomes (linearly) unstable, the speed can even be negative if the optimal speed function V_{op} is not positively defined. To this end, we impose the following constraint in the numerical implementation: $V_{op}^+ = \max(0, V_{op})$. This will guarantee that the stochastic speed is pushed towards the non-negative value in the low speed regime. In the following sections, we will show that the effect of the stochastic part (i.e. the standard deviation of the acceleration) on traffic stability vanishes in the free-flow traffic regime.

Remark 1. *If we set $V_{op}(s_n(t)) = v_c$ as in the case of the model of Laval et al. (2014), equation (12) follows a standard CIR process, from which the solution for $v_n(t)$ has the Gaussian distribution with asymptotic mean and variance:*

$$E[v_n(t)] = v_0 e^{-\beta t} + v_c (1 - e^{-\beta t}) \quad (13)$$

$$Var[v_n(t)] = \frac{v_0 \sigma_0^2}{\beta} (e^{-\beta t} - e^{-2\beta t}) + \frac{v_c \sigma_0^2}{2\beta} (1 - e^{-\beta t})^2 \quad (14)$$

and at the equilibrium state:

$$\lim_{t \rightarrow \infty} E[v_n(t)] = v_c; \quad \lim_{t \rightarrow \infty} Var[v_n(t)] = \frac{v_c \sigma_0^2}{2\beta} \quad (15)$$

In the CIR process, at the equilibrium state, unlike the model of Laval et al. (2014), the speed variance also depends on the critical speed v_c . Note that, due to the contribution of $\sqrt{v_n(t)}$ in the stochastic part of the CIR-like model, the unit of σ_0 is different between our model and the model of Laval et al. (2014).

3. Linear stochastic stability

In order to understand the stability of the model in response to the multiplicative white noise (i.e. the Brownian motions), let us adopt the linear analysis method. In principle, the linear stability method has been used widely in traffic flow literature to derive the conditions influencing the long-wavelength instabilities of traffic flow. We will adopt such method to our stochastic car-following model equation (12). The stochastic model of Treiber and Kesting (2017) shows that stochasticity does not affect the linear stability of traffic flow. Whereas empirical results in Jiang et al. (2018) indicated that the stochastic nature of drivers does destabilize traffic flow at low speed, where the deterministic model shows a stable traffic pattern. This section describes a first attempt to derive the general linear stochastic stability condition of stochastic car-following models, which is consistent with the empirical findings in Jiang et al. (2018).

More specifically, in the stationary situation, the speed of the considered vehicle is given by $v_n = v_{n-1} = \dots = v_e$ and the gap is given by $s_n = s_{n-1} = \dots = s_e$ which is calculated from a mean fundamental diagram $v_e = V_{op}(s_e)$. Now let δv_n and δs_n denote the small deviation of the speed and gap around the stationary situation: $v_n = v_e + \delta v_n$ and $s_n = s_e + \delta s_n$. First order Taylor expansion of equation (12) leads to a linear stochastically perturbed evolution equation:

$$d\delta v_n(t) = -\beta \delta v_n(t) dt + \beta V'_{op} \delta s_n(t) dt + \frac{\sigma_0}{2\sqrt{v_e}} \delta v_n(t) dW(t), \quad (16)$$

Note, by definition, we have:

$$d\delta s_n(t) = (\delta v_{n-1}(t) - \delta v_n(t)) dt \quad (17)$$

3.1. Local stability condition

In this section, we will study the evolution of the gap and speed deviation, i.e. δs_n and δv_n , given model parameters and dissipation parameters via a local stability analysis. In principle, the local stability describes how a driver recovers from a small disturbance in real-life traffic and returns to his/her steady state over time. That is the local stability is guaranteed if the gap and speed fluctuations of the followers decrease over time, or at least, do not amplify. To derive the local stability conditions, we adopt the Lyapunov stability theory, which makes use of a Lyapunov function $V(\mathbf{U})$. If we can find a non-negative function $V(\mathbf{U})$ that always decreases along trajectories of the system, a locally stable equilibrium state can be found.

Note for the local stability analysis, the leader's speed is fixed, and generally taken as a constant value so we set $\delta v_{n-1} = 0$, and we consider the stability of the follower w.r.t. the leading vehicle behavior (that is why it is called local stability). Thus mathematically system of equations (16)

and (17) can be written as the following linear stochastic ordinary differential equations (SODEs):

$$d\mathbf{U}(t) = \mathbf{F}\mathbf{U}(t)dt + \mathbf{G}\mathbf{U}(t)d\mathbf{W}(t) \quad (18)$$

where

$$\mathbf{U} = \begin{bmatrix} \delta s_n \\ \delta v_n \end{bmatrix}, \quad \mathbf{F} = \begin{bmatrix} 0 & -1 \\ \beta V'_{op} & -\beta \end{bmatrix}, \quad \mathbf{G} = \begin{bmatrix} 0 & 0 \\ 0 & \gamma \end{bmatrix} \quad (19)$$

with $\gamma = \frac{\sigma_0}{2\sqrt{v_e}}$.

To follow the standard derivation of the Lyapunov stability condition in Mao (2008), we have the following definition:

Definition 1. Let Φ denote the family of all continuous non-decreasing functions ϕ such that $\phi(0) = 0$ and $\phi(r) > 0$ if $r > 0$. The trivial solution of the stochastic system (18) is said to be locally stochastic stable if there exist a Lyapunov function $V(\mathbf{U}(t))$ satisfying:

$$V(\mathbf{U}(t)) \geq \phi(|\mathbf{U}(t)|), \quad \phi \in \Phi \quad (\text{i.e. positive definite}) \quad (20)$$

$$LV(\mathbf{U}(t)) = V_1(\mathbf{U}(t))\mathbf{F}\mathbf{U}(t) + \frac{1}{2} \text{Tr} [(G\mathbf{U}(t))^T V_2(\mathbf{U})G\mathbf{U}(t)] \leq 0 \quad (\text{i.e. negative definite}) \quad (21)$$

where

$$V_1(\mathbf{U}) = \begin{bmatrix} \frac{\partial V}{\partial \delta s_n} \\ \frac{\partial V}{\partial \delta v_n} \end{bmatrix}, \quad V_2(\mathbf{U}) = \begin{bmatrix} \frac{\partial^2 V}{\partial \delta s_n^2} & \frac{\partial^2 V}{\partial \delta s_n \partial \delta v_n} \\ \frac{\partial^2 V}{\partial \delta v_n \partial \delta s_n} & \frac{\partial^2 V}{\partial \delta v_n^2} \end{bmatrix}$$

Then we have the following theorem:

Theorem 1. The stochastic car-following model (12) is locally stable if :

$$\sigma_0^2 \leq 8\beta v_e \quad (22)$$

Proof. For the system (18), we define a Lyapunov function as:

$$V(\mathbf{U}(t)) = \mathbf{U}^T(t)\mathbf{Q}\mathbf{U}(t) \quad (23)$$

with

$$\mathbf{Q} = \begin{bmatrix} \beta V'_{op} & 0 \\ 0 & 1 \end{bmatrix} \quad (24)$$

which leads to $V(\mathbf{U}(t)) = \beta V'_{op} \delta s_n^2(t) + \delta v_n^2(t)$ and

$$LV(\mathbf{U}(t)) = \left(-2\beta + \frac{\sigma_0^2}{4v_e} \right) \delta v_n^2(t) \quad (25)$$

It is clear that, $V(\mathbf{U}(t)) \geq \lambda_{min}(\mathbf{Q}) \|\mathbf{U}(t)\|^2$ where $\lambda_{min}(\mathbf{Q})$ denotes the smallest eigenvalues of the matrix \mathbf{Q} . Therefore, condition (20) is satisfied. To guarantee $LV(\mathbf{U}(t)) \leq 0$, i.e. condition (21), we need: $\sigma_0^2 \leq 8\beta v_e$ \square

When $\sigma_0 = 0$ (i.e. the original OVM), the system is locally stable. However, large noise clearly destabilizes the local stability of the system.

3.2. String stability condition

The string stability considers how a small perturbation in the gap and speed of the leader affect the gap and speed of all the followers. The string stability of deterministic car-following models has been studied extensively in the literature (see example, Ngoduy (2013a) and references there-in). The contribution of this section is to derive the linear stability condition taking into account the multiplicative white noisy terms. Let $\delta s_n = \mathcal{S}e^{i\omega n + \lambda t}$ and $\delta v_n = \mathcal{M}e^{i\omega n + \lambda t}$, where \mathcal{S} and \mathcal{M} are constants, then the system of equations (16) and (17) is also written as the following linear SODEs:

$$d\mathbf{U}(t) = \mathbf{F}\mathbf{U}(t)dt + \mathbf{G}\mathbf{U}(t)d\mathbf{W}(t) \quad (26)$$

where $\mathbf{U}(t)$ and \mathbf{G} are defined as above, while

$$\mathbf{F} = \begin{bmatrix} 0 & e^{-i\omega} - 1 \\ \beta V'_{op} & -\beta \end{bmatrix} \quad (27)$$

In the literature of stochastic process, there is a wide spectrum of stochastic stability analysis for both continuous and discrete stochastic differential equations (Kushner, 1971). In this paper we expand these ideas to our proposed stochastic car-following model (12) while focusing on almost sure stability, moment (i.e. 2nd order) stability (which is also called mean square stability), and the relationship between them. To follow the text in Evans (2014), the following definitions are used for the stochastic stability analysis:

Definition 2. *The stochastic system is said to be almost surely linearly stochastically stable (i.e. asymptotically stochastically stable in the large) if the solution of equation (26) has the following convergence property:*

$$\lim_{t \rightarrow \infty} \|\mathbf{U}(t)\| = 0 \text{ with probability } 1 \quad (28)$$

It has been shown in literature of SDEs (e.g. Evans (2014), Gardiner (2009), Mao (2008)) that condition (28) is equivalent to:

$$\Re\{\mathbf{F}^*\} = \Re\{\mathbf{F} - 0.5 \|\mathbf{G}\|^2\} \leq 0 \quad (29)$$

where $\Re\{\mathbf{F}^*\}$ denotes the real parts of the eigenvalues of the Jacobian matrix $\mathbf{F}^* = \mathbf{F} - 0.5 \|\mathbf{G}\|^2$, with \mathbf{F} being defined in (27).

Definition 3. *The stochastic system is said to be mean square stable (i.e. asymptotically stochastically mean square stable) if the solution of equation (26) has the following convergence property:*

$$\lim_{t \rightarrow \infty} E [\|\mathbf{U}(t)\|^2] = 0 \quad (30)$$

To follow the literature of SDEs (e.g. Evans (2014), Gardiner (2009), Mao (2008)), condition (30) is equivalent to:

$$\Re\{\mathbf{F}\} + 0.5 \|\mathbf{G}\|^2 \leq 0 \quad (31)$$

Note that if $\mathbf{G} = 0$ conditions (29) and (31) are equivalent to the linear stability condition of the deterministic OVM, i.e. $\Re\{\mathbf{F}\} \leq 0$. Then we have the following theorem:

Theorem 2. *The stochastic car-following model (12) is almost sure stable if:*

$$\sigma_0^2 \leq 8v_e \left(\beta - \sqrt{2\beta V'_{op}} \right) \quad (32)$$

Obviously, condition (32) is stricter than the local stability condition.

Proof. It is straightforward to show that the eigenvalues of the Jacobian matrix \mathbf{F}^* is the solutions of the following characteristic equation:

$$\lambda^2 + \left(\beta - \frac{\sigma_0^2}{8v_e} \right) \lambda - \beta V'_{op} (e^{-i\omega} - 1) = 0 \quad (33)$$

Let us expand λ in a power series solution $\lambda = i\omega\lambda_1 + \omega^2\lambda_2 + \dots$ where λ_1 and λ_2 are real coefficients. Let us substitute this expansion into equation (33) and expand the exponential terms to the second order, and set the first order ($\mathcal{O}(\omega)$) and the second order ($\mathcal{O}(\omega^2)$) terms to zero. After a rather lengthy but straightforward algebraic calculation we have the following solutions:

$$\lambda_1 = -\frac{\beta V'_{op}}{\beta^*}, \quad (34)$$

and

$$\lambda_2 = \frac{1}{\beta^*} \left(\lambda_1^2 - \frac{\beta V'_{op}}{2} \right) \quad (35)$$

where $\beta^* = \beta - \frac{\sigma_0^2}{8v_e}$.

Condition (29) holds if $\lambda_1 \leq 0$ and $\lambda_2 \leq 0$. It is obvious that $\lambda_1 \leq 0$ leads to $\beta^* \leq 0$. This is equivalent to $\sigma_0^2 \leq 8\beta v_e$. Whereas $\lambda_2 \leq 0$ leads to:

$$\sigma_0^2 \leq 8v_e \left(\beta - \sqrt{2\beta V'_{op}} \right) \quad (36)$$

which also satisfies: $\sigma_0^2 \leq 8\beta v_e$. □

Theorem 3. *The stochastic car-following model (12) is mean square stable if:*

$$\sigma_0^2 \leq \frac{4v_e V'_{op}}{\beta} \left(\beta - 2V'_{op} \right) \quad (37)$$

Proof. Following the proof in Theorem 2, the eigenvalues of the Jacobian matrix \mathbf{F} is the solutions of the following characteristic equation:

$$\lambda^2 + \beta\lambda - \beta V'_{op} (e^{-i\omega} - 1) = 0 \quad (38)$$

which lead to the following solutions:

$$\lambda_1 = -V'_{op} \quad (39)$$

and

$$\lambda_2 = \frac{1}{\beta} \left(\lambda_1^2 - \frac{\beta V'_{op}}{2} \right) \quad (40)$$

Since $\lambda_1 \leq 0$, condition (31) holds if and only if $\lambda_2 + 0.5\gamma^2 \leq 0$ which is equivalent to:

$$\sigma_0^2 \leq \frac{4v_e V'_{op}}{\beta} (\beta - 2V'_{op}) \quad (41)$$

□

Remark 2. When $\sigma_0 = 0$, both conditions (29) and (31) become $\beta \geq 2V'_{op}$, which is the stability condition of the original OVM.

Remark 3. The almost sure stability condition also implies the local stability condition. This is true for both deterministic and stochastic OVM.

Remark 4. For the stochastic car-following model (12), the mean square stability condition (i.e. $\Re\{\mathbf{F}\} + 0.5 \|\mathbf{G}\|^2 \leq 0$) also implies the almost sure stability condition since $\Re\{2\mathbf{F} - \|\mathbf{G}\|^2\} \leq 2\Re\{\mathbf{F}\} + \|\mathbf{G}\|^2 \leq 0$, which leads to $\Re\{\mathbf{F} - 0.5 \|\mathbf{G}\|^2\} \leq 0$.

4. Model performance

The proposed model is numerically simulated using a standard Euler-Maruyama scheme. Details of the discretization is given in the Appendix. This section illustrates numerically the effects of the model parameters on the (linear) traffic stability and the performance of the proposed model in replicating real-world traffic data.

4.1. Stochastic linear stability diagrams

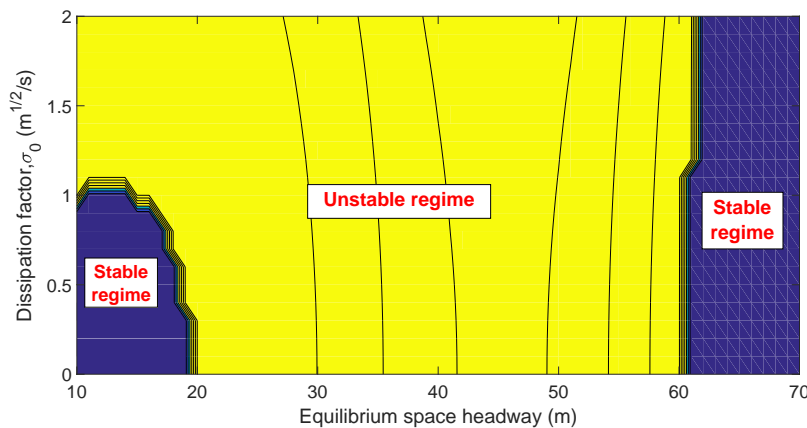


Figure 1: Stochastic almost sure stability diagram for a range of σ_0

Let us study the stability diagrams for various values of σ_0 against a range of the initial equilibrium space headway in Figures 1 and 2. In these figures, the following model parameters are used: $\beta = 0.5s^{-1}$, $v_0 = 25\text{m/s}$, $s_c = 20\text{m}$, and $\alpha = 2$. The unstable regime covers all the values of σ_0 and s_e so that the stability conditions (32) and (37) are violated (i.e. yellow regime), respectively. Whereas, in the stable regime the stability conditions (32) and (37) hold (i.e. dark-blue regimes), respectively. It is seen in both figures that when traffic is in the free-flow stable regime (i.e. when the space-headway is relatively large), the stochastic factor has insignificant

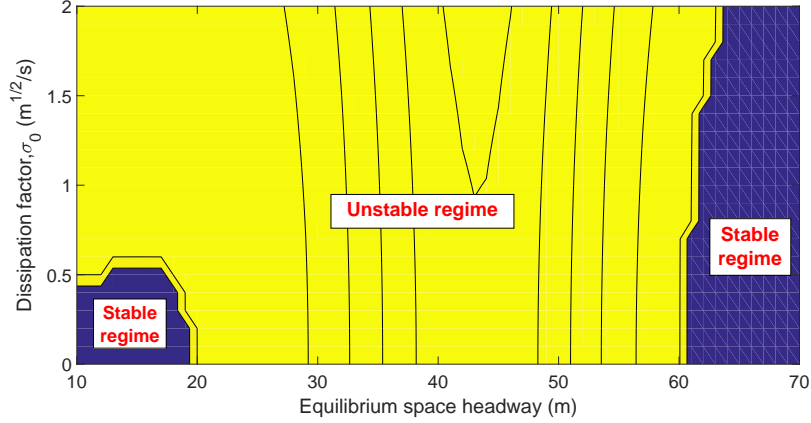
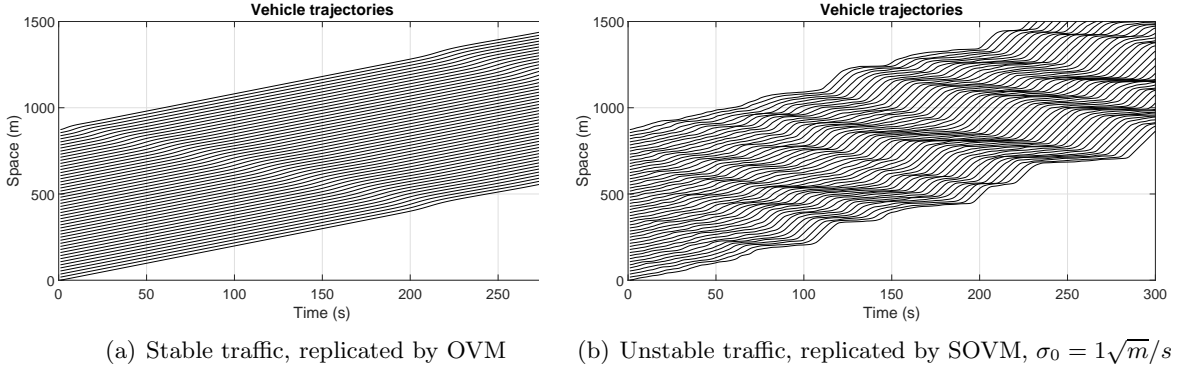


Figure 2: Stochastic mean square stability diagram for a range of σ_0



(a) Stable traffic, replicated by OVM

(b) Unstable traffic, replicated by SOVM, $\sigma_0 = 1\sqrt{m}/s$

Figure 3: Trajectories of 50 vehicles under the initial equilibrium space of 18m

impact on the stability of traffic flow. However, when traffic is in the congested stable regime (i.e. the space headway is relatively small, $s_e \leq 20\text{m}$), increasing stochastic factor tends to destabilize significantly traffic flow. This has been confirmed from empirical investigations in Jiang et al. (2018): a small perturbation dies out in the deterministic model (i.e. traffic is stable), whereas the stochastic nature of traffic flow leads to the instability at low speed conditions. For example, in Figure 1, when $\sigma_0 \geq 1\sqrt{m}/s$ traffic is unstable for all space headway below 60m. Whereas in Figure 2 when $\sigma_0 \geq 0.5\sqrt{m}/s$ traffic is unstable for all space headway below 60m. It is also clear that the stable regimes for almost sure stability condition are larger than those for mean square stability condition (i.e. this conforms to our Remark 3).

Figure 3 shows the trajectories of 50 vehicles, replicated by the OVM (Fig. 3(a)) and the SOVM (Fig. 3(b)) using the above model parameters and the initial equilibrium space headway $s_e = 18\text{m}$. With these model settings, the stability condition of the OVM is $\beta - 2V'_{op} = 0.05 > 0$ which indicates a stable traffic condition at the low equilibrium speed. In contrast, the right-hand side of the stability condition (37) of the SOVM is $0.1872 < \sigma_0^2 = 1$ indicating an unstable traffic condition at the low equilibrium speed.

4.2. Model calibration with real data

In this section, we briefly describe the calibration results of the proposed model against the real data. More extensive model verification is given in a separate paper (Lee et al., 2019). The model parameters to be calibrated are:

- Free-flow speed v_0 (m/s)
- Reaction coefficient β (1/s)
- Critical headway s_c (m)
- Constant coefficient α (dimensionless)
- Dissipation coefficient σ_0 (\sqrt{m}/s)

Note that, similar to the model of Laval et al. (2014), our proposed model only generates one additional parameter from the original OVM, that is the dissipation coefficient σ_0 .

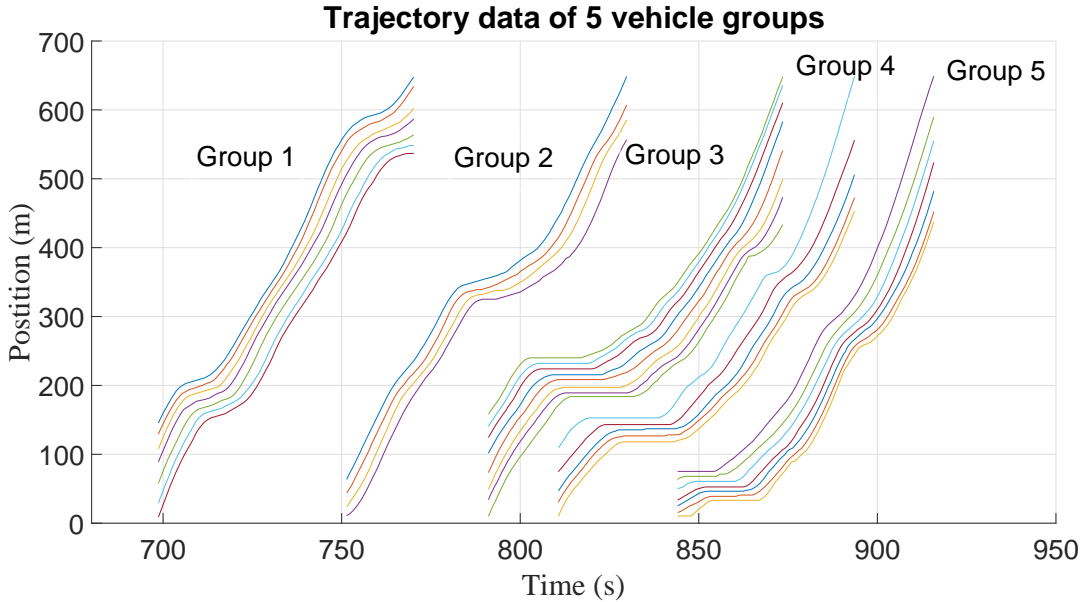


Figure 4: Trajectory data used for the model calibration

To verify the effectiveness of the proposed model, real vehicle trajectory data set collected in a U.S. freeway. The dataset and detailed information were provided by the Federal Highway Administrations Next Generation Simulation (NGSIM). The trajectory data at different time periods are described in the Figure 4. We select the trajectory data in the 3rd vehicle group (i.e. at 800s) where there was a substantial traffic congestion at position 200m, for our calibration. To calibrate the model, a standard genetic algorithm is used for our purposes where 100 replications will be used in the stochastic simulation. The mean of the individual vehicle speed is used to compare with the observed individual vehicle speed where the total mean squared errors between the model output and the data is used as a performance index (PI):

$$z = \sum_{j=1}^J \sqrt{\frac{1}{K} \sum_{k=1}^K [v_j(k|\boldsymbol{\pi}) - \tilde{v}_j(k)]^2} \quad (42)$$

where $k \in K$ is time step, $v_j(k|\boldsymbol{\pi})$ denotes the simulated speed of vehicle j at time step k given the model parameter $\boldsymbol{\pi} = [v_0 \ \beta \ s_c \ \alpha \ \sigma_0]$. In contrast, $\tilde{v}_j(k)$ is the measured speed of vehicle j at time step k .

Table 1: Optimal model parameters obtained from the GA.

Free-flow speed $v_0(m/s)$	Reaction coefficient $\beta (1/s)$	Critical headway $s_c (m)$	Constant coefficient α (dimensionless)	Dissipation coefficient $\sigma_0 (\sqrt{m}/s)$
17.65	0.65	8.20	1.85	0.88

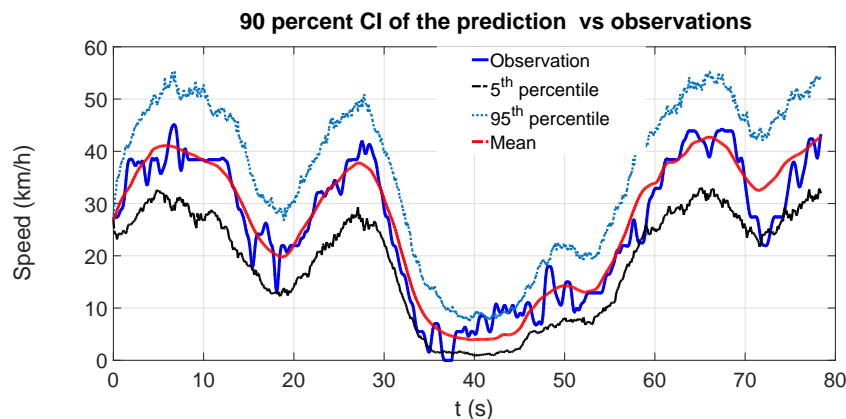


Figure 5: Model prediction vs observation

Table 1 shows the optimal model parameters obtained after 30 optimization iterations. Figure 5 shows the predicted speed of the 2nd vehicle against the observed values. In Figure 5, the upper and lower bound show the trailing vehicle speed (90% confidence interval-CI). The solid blue line shows the observed speed while the dashed red line shows the mean of the predicted speed. Figure 5 illustrates that the observed speed fits well to the range of the stochastic model output at 90% CI and matches well to the mean of the model output. It is seen that the observed speed is always within the upper and lower bound of the predicted speed (at 90% confidence interval). Moreover, the variance of the predicted stochastic speed is relatively low when the speed is low (e.g. at time $t = 40s$). A wide range of the predicted speeds at a certain time instant are described in Figure 6, which conforms to a Gaussian distribution with the mean value being identified from Figure 5 (i.e. approximately $40km/h$).

5. Concluding remarks

The mathematical framework of stochastic car-following models developed in this study can deal with uncertain human perception. This is achieved by integrating the OVM in the stochastic equation. The proposed model is a first attempt to allow us to understand analytically how human errors can be responsible for traffic instabilities where the deterministic part is stable. This is

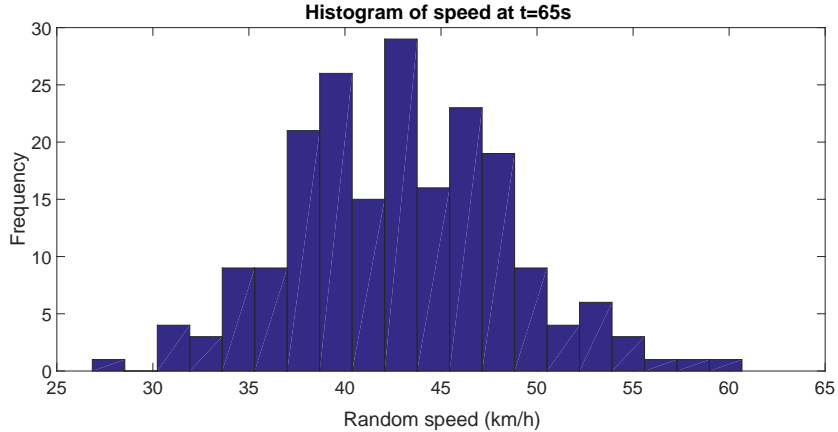


Figure 6: Distribution of the predicted speed at $t = 65s$

achieved by relaxing the assumptions of constant dissipation parameter and constant optimal speed in the stochastic acceleration of Laval et al. (2014). Moreover, the formulation of the proposed model follows an extended CIR stochastic process which consequently enhances non-negative speed values for arbitrary model parameters. The model calibration results show good consistency with the trajectory data collected in a US freeway (i.e. NGSIM data). Our concurrent research is to extend the proposed method for multi-lane traffic dynamics, in which the lane-changing probability is continuously estimated using a deep learning method (Lee et al., 2019).

Finally, we would like to mention that Connected and Autonomous vehicles (CAVs) have been verified to significantly improve traffic efficiency. However, there is still a long lifespan for heterogeneous traffic flow consisting of both human-driven vehicles and CAVs. Thus a deep understanding of the mixed traffic dynamics including both CAVs and human-driven vehicles is critical to the traffic stability issues for the deployment of CAVs in the near future. Many efforts have been made to study the impact of CAVs on traffic flow instability such as Ngoduy (2013a,b), Talebpour and Mahmassani (2016), Wang et al. (2017). Recently, Jia et al. (2019) have proposed a novel model to consider the behavior of the CAVs in a heterogeneous platoon in detail but ignored the stochasticity of the drivers in the human-driven vehicles. In our future work, by introducing the proposed SOVM to model the stochastic human behavior, we hope to extend our approach to study the impact of CAVs on traffic instability under more realistic traffic flow situations.

Appendix A. Discrete-time stochastic model

It is straightforward to formulate our model in the following form for numerical simulation.

$$d\mathbf{u} = \mathbf{A}(\mathbf{u}, t) dt + \mathbf{B}(\mathbf{u}, t) d\mathbf{W}(t) \quad (\text{A.1})$$

where

$$\mathbf{u}(t) = \begin{bmatrix} x_1(t) \\ \vdots \\ x_N(t) \\ v_1(t) \\ \vdots \\ v_N(t) \end{bmatrix}, \quad \mathbf{A}(\mathbf{u}, t) = \begin{bmatrix} v_1(t) \\ \vdots \\ v_N(t) \\ \beta(V_{op}(s_1(t)) - v_1(t)) \\ \vdots \\ \beta(V_{op}(s_N(t)) - v_N(t)) \end{bmatrix} \quad (\text{A.2})$$

and

$$\mathbf{B}(\mathbf{u}, t) = \begin{bmatrix} \mathbf{O} & \mathbf{O} \\ \mathbf{O} & \mathbf{C}(\mathbf{u}, t) \end{bmatrix}, \quad \mathbf{W}(t) = \begin{bmatrix} 0 \\ \vdots \\ 0 \\ W_1(t) \\ \vdots \\ W_N(t) \end{bmatrix} \quad (\text{A.3})$$

with

$$\mathbf{C}(\mathbf{u}, t) = \begin{bmatrix} \sigma_0\sqrt{v_1(t)} & 0 & \dots & 0 \\ 0 & \sigma_0\sqrt{v_2(t)} & \dots & 0 \\ \vdots & \vdots & \ddots & \vdots \\ 0 & 0 & \dots & \sigma_0\sqrt{v_N(t)} \end{bmatrix} \quad \text{for our proposed model} \quad (\text{A.4})$$

or

$$\mathbf{C}(\mathbf{u}, t) = \begin{bmatrix} \sigma_0 & 0 & \dots & 0 \\ 0 & \sigma_0 & \dots & 0 \\ \vdots & \vdots & \ddots & \vdots \\ 0 & 0 & \dots & \sigma_0 \end{bmatrix} \quad \text{for Laval et al.-type model} \quad (\text{A.5})$$

The models are simulated by using an explicit Euler-Maruyama scheme. The discretization of the SOVM is

$$\mathbf{u}(k+1) - \mathbf{u}(k) = \mathbf{A}(\mathbf{u}(k)) \Delta t + \mathbf{B}(\mathbf{u}(k)) \sqrt{\Delta t} \mathbf{w}(k+1) \quad (\text{A.6})$$

$$\mathbf{w}(k) = \begin{bmatrix} 0 \\ \vdots \\ 0 \\ w_1(k) \\ \vdots \\ w_N(k) \end{bmatrix}, \quad w_n(k) \sim \mathcal{N}(0, 1) \quad (\text{A.7})$$

If we change σ_0 by δ , the change in the speed in a time step is:

$$\Delta v_n(k+1) = \delta\sqrt{\Delta t}w_n(k+1), \text{ for model of Laval et al. (2014)} \quad (\text{A.8})$$

$$\Delta v_n(k+1) = \delta\sqrt{v_n(k)}\sqrt{\Delta t}w_n(k+1), \text{ for our model} \quad (\text{A.9})$$

It shows that the effect of a change in σ_0 in our model is insignificant when speed is low. It is also worth mentioning that the change is greatly affected by the random term.

References

- Bando, M., Hasebe, K., Nakayama, A., Shibata, A., Sugiyama, Y., 1995. Dynamical Model of Traffic Congestion and Numerical Simulation. *Physical Review E* 51, 1035–1042.
- Cox, J. C., Ingersoll, J. E., Ross, S. A., 1985. A Theory of the Term Structure of Interest Rates. *Econometrica* 53, 385–407.
- Evans, L., 2014. An introduction to stochastic differential equations. AMS, USA.
- Gardiner, C., 2009. *Stochastic Methods: A Handbook for the Natural and Social Sciences*. Springer, Germany.
- Jabari, S., Zheng, J., Liu, H., 2014. A probabilistic stationary speed-density relation based on Newell's simplified car-following model. *Transportation Research Part B* 68, 205–2234.
- Jabari, S. E., Liu, H. X., 2012. A stochastic model of traffic flow: Theoretical foundations. *Transportation Research Part B* 46, 156–174.
- Jabari, S. E., Liu, H. X., 2013. A stochastic model of traffic flow: Gaussian approximation and estimation. *Transportation Research Part B* 47, 15–41.
- Jabari, S. E., Zheng, F., Liu, H., Filipovska, M., 2018. Stochastic lagrangian modeling of traffic dynamics. In: *The 97th Annual Meeting of the Transportation Research Board, Washington, DC*. No. 18-04170.
- Jia, D., Ngoduy, D., Vu, H., 2019. A multiclass microscopic model for heterogeneous platoon with vehicle-to-vehicle communication. *Transportmetrica B* 7, 448–472.
- Jiang, R., Jin, C., Zhang, H., Huang, Y., Tiang, J., Wang, W., M.B., H., Wang, H., Jia, B., 2018. Experimental and empirical investigations of traffic instability. *Transportation Research Part C* 94, 83–98.
- Jiang, R., Wu, Q., Zhu, Z., 2002. Full Velocity Difference Model for a Car-Following Theory. *Physical Review E* 64, 017101–017104.
- Kushner, H., 1971. *Introduction to Stochastic Control*. Holt and Rinehart and Winston.
- Laval, J. A., Chilukuri, B. R., 2013. The Distribution of Congestion on a Class of Stochastic Kinematic Wave Models. *Transportation Science* 48, 217–224.
- Laval, J. A., Toth, C. S., Zhou, Y., 2014. A parsimonious model for the formation of oscillations in car-following models. *Transportation Research Part B* 70, 228–238.
- Lee, S., Ngoduy, D., Keyvan-Ekbatani, M., 2019. Integrated deep learning and stochastic car-following model for traffic dynamics on multi-lane freeways. *Transportation Research Part C* submitted.
- Li, J., Chen, Q., Wang, H., Ni, D., 2012. Analysis of LWR model with fundamental diagram subject to uncertainties. *Transportmetrica A: Transport Science* 8, 387–405.
- Mahnke, R., Kaupuzs, J., Lubashevsky, I., 2009. *Physics of stochastic processes: how randomness acts in time*. John Wiley & Sons.
- Mao, X., 2008. *Stochastic differential equations and applications*. Horwood, Chichester.
- Newell, F. G., 2002. A simplified car-following theory: a lower order model. *Transportation Research Part B* 36, 195–205.
- Ngoduy, D., 2011. Multiclass first-order traffic model using stochastic fundamental diagrams. *Transportmetrica* 7, 111–125.
- Ngoduy, D., 2013a. Analytical studies on the instabilities of heterogeneous intelligent traffic flow. *Communications in Nonlinear Science and Numerical Simulation* 18, 2699–2706.
- Ngoduy, D., 2013b. Instabilities of cooperative adaptive cruise control traffic flow: a macroscopic approach. *Communications in Nonlinear Science and Numerical Simulation* 18, 2838–2851.
- Sumalee, A., Zhong, R. X., Pan, T. L., Szeto, W. Y., 2011. Stochastic cell transmission model (SCTM): a stochastic dynamic traffic model for traffic state surveillance and assignment. *Transportation Research Part B* 45, 507–533.
- Talebpour, A., Mahmassani, H., 2016. Influence of connected and autonomous vehicles on traffic flow stability and throughput. *Transportation Research Part C* 71, 143–163.

- Tian, J., Jiang, R., Jia, B., Gao, Z., Ma, S., 2016b. Empirical analysis and simulation of the concave growth pattern of traffic oscillations. *Transportation Research Part B* 93, 338–354.
- Tian, J., Jiang, R., Li, G., Treiber, M., Jia, B., Zhu, C., 2016a. Improved 2D intelligent driver model in the framework of three-phase traffic theory simulating synchronized flow and concave growth pattern of traffic oscillations. *Transportation Research Part F* 41, 55–65.
- Tordeux, A., Roussignol, M., Lebacque, J. P., Lassarre, S., 2014. A stochastic jump process applied to traffic flow modelling. *Transportmetrica A: Transport Science* 10, 350–375.
- Treiber, M., Kesting, A., 2013. *Traffic Flow Dynamics*. Springer, Germany.
- Treiber, M., Kesting, A., 2017. The Intelligent Driver Model with stochasticity - New insights into traffic flow oscillations. *Transportation Research Part B* 23, 174–187.
- Treiber, M., Kesting, A., Helbing, D., 2005. Delays, inaccuracies and anticipation in microscopic traffic model. *Physica A* 360, 71–88.
- Treiber, M., Kesting, A., Helbing, D., 2006. Understanding widely scattered traffic flows, the capacity drop, and platoon as effects of variance-driven time gaps. *Physical Review E* 74, 0161231–0161239.
- Uhlenbeck, G. E., Ornstein, L. S., 1930. On the theory of Brownian Motion. *Physical Review* 36, 823–841.
- Wang, R., Li, Y., Work, D., 2017. Comparing traffic state estimators for mixed human and automated traffic flows. *Transportation Research Part C* 78, 95–110.
- Yeo, H., Skabardonis, A., 2009. Understanding stop-and-go traffic in view of asymmetric traffic theory. *International Symposium on Transportation and Traffic Theory* , 99–115.
- Yuan, K., Laval, J., Knoop, V., Jiang, R., Hoogendoorn, S., 2018. A geometric Brownian motion car-following model: towards a better understanding of capacity drop. *Transportmetrica B* in press.
- Zhong, R. X., Sumalee, A., Pan, T. L., Lam, W. H. K., 2013. Stochastic cell transmission model for traffic network with demand and supply uncertainties. *Transportmetrica A: Transport Science* 9, 567–602.
- Zhou, M., Qu, X., Li, X., 2017. A recurrent neural network based microscopic car following model to predict traffic oscillation. *Transportation Research Part C* 84, 245–264.